Available online at www.sciencedirect.com
ScienceDirect
International Journal of Heat and Mass Transfer 50 (2007) 3411–3421
International Journal of HEAT and MASS TRANSFER
www.elsevier.com/locate/ijhmt

Analytical solution of gaseous slip flow in long microchannels

Nishanth Dongari [a], Abhishek Agrawal [b], Amit Agrawal [a,*]

[a] Department of Mechanical Engineering, Indian Institute of Technology Bombay, Powai, Mumbai 400 076, India
[b] ABB Lummus Global B. V., 2nd Floor, Infinity Tower-B, Gurgaon 122 002, India

Received 4 April 2006; received in revised form 20 September 2006
Available online 11 April 2007

Abstract

In this paper we provide solution of the Navier–Stokes equations for gaseous slip flow in long microchannels with a second-order accurate slip boundary condition at the walls. The obtained solution is general enough to allow evaluation of various slip models proposed in the literature. We compare our solution against the first-order accurate slip boundary condition and show that the solution has a weak dependence on Reynolds number, which was neglected in the earlier theory. It is emphasized that first-order slip models do not predict the "Knudsen paradox" (appearance of a minima in normalized volume flux at Knudsen number approximately unity), or a change in curvature of centerline pressure at Knudsen numbers of 0.16. A comparison with Boltzmann's solution suggests that the derived solution agrees reasonably well up to Knudsen number approximately 5, which shows that the validity of Navier–Stokes to rarefied gases can possibly be increased by using a high order slip boundary condition and proper choice of the slip coefficients. This result is significant from the perspective of numerical simulations of rarefied gases.

1. Introduction

Study of flow through microchannels has gained interest because of potential applications of microdevices in engineering, medical, and other scientific areas. These devices would invariably involve fluid flow and therefore a clear understanding of microfluidics is imperative. The flow of liquid in a microchannel is different from that of a gas in the same microchannel (see, e.g., Gad-el-Hak [1]). Whereas standard results usually apply with liquid flow, this is not the case with gases: the most noticeable difference between micro and macro domains with gases is presence of slip at the solid interfaces. This can be seen by considering air flow under standard conditions ($\lambda \approx 70$ nm) through a 5 μm channel which gives a Knudsen number, Kn (defined as the mean free path of the gas, λ, divided by the hydraulic diameter) of 0.007 which is well within the slip regime ($10^{-3} < Kn < 10^{-1}$; Schaaf and Chambre [2]). The slip velocity therefore needs to be properly specified in such analysis and simulations in order to obtain meaningful results.

The Knudsen number is large if either the mean free path of the gas is large or the characteristic dimension of the channel is small. The former can be accomplished by reducing the pressure in the channel, i.e., by working under rarefied condition, whereas the latter can occur in microdevices. Rarefied gases, especially in the free-molecular regime ($Kn > 10$), have been studied with interest to space applications. The theory for free-molecular, and to some extend the transition regime ($10^{-1} < Kn < 10$), is well developed. On the other hand in microdevices, as illustrated by the above example, internal slip flow is expected to be commonly encountered; the slip regime therefore needs to be better understood and the present work pertains to this flow regime. The connection between rarefied gases and gas flow through microdevices should be kept in mind; because of this commonality, the validity of our results extend to both micro and macro domains under similar values of Knudsen and Reynolds numbers.

The theory for incompressible, isothermal laminar flow in a macrochannel is well known due to the inherent

* Corresponding author. Tel.: +91 22 2576 7516; fax: +91 22 2572 6875.
E-mail address: amit.agrawal@me.iitb.ac.in (A. Agrawal).

0017-9310/$ - see front matter © 2007 Elsevier Ltd. All rights reserved.
doi:10.1016/j.ijheatmasstransfer.2007.01.048

Nomenclature

A	cross-sectional of the channel (m^2)
b	empirical parameter (see Eq. (3))
C_1	first-order slip coefficient
C_2	second-order slip coefficient
c_s	speed of sound (m/s)
D_h	hydraulic diameter of a channel ($=\frac{4A}{\text{Perimeter}}$) (m)
f	friction factor (see Eq. (21))
H	height of the channel (m)
Kn	Knudsen number ($=\lambda/2H$)
Kn_0	Knudsen number at reference point z_0
L	channel length (m)
$\dot{m}$	mass flux per unit depth (kg/m s)
n	unit normal to the surface ($=y/H$)
p	pressure (Pa)
p_0	pressure at reference position z_0 (Pa)
Q	normalized volume flux (see Eq. (23))
R	specific gas constant (J/kg K)
Re	Reynolds number
T	temperature (K)
u	longitudinal velocity (m/s)
$\bar{u}$	cross-section average velocity (m/s)
u_g	slip velocity at the wall (m/s)
u_λ	longitudinal velocity at a distance λ from the wall (m/s)
v	lateral component of velocity (m/s)
y	lateral coordinate (m)
z	streamwise coordinate (m)
z_0	reference position (m)

Greek symbols

β	non-dimensional constant (see Eq. (13))
χ	non-dimensional constant (see Eq. (14))
γ	pressure ratio across the channel
λ	mean free path of a gas (m)
μ	dynamic viscosity (kg/m s)
ρ	density (kg/m^3)
σ	tangential momentum accommodation factor
τ_w	shear stress at the wall ($kg/m\ s^2$)
ϱ	conductance of the channel (see Eq. (22))
ζ	slip length (m)

Subscripts

g	gas
s	control surface (at a distance $\lambda/2$ from the wall)
w	wall

simplicity of the problem. This is however not the case with microchannels – the difficulty stems from the fact that the flow is compressible and the slip at the walls has to be appropriately modelled. Development of a comprehensive theory, besides being of fundamental importance, will be useful for benchmarking experimental and numerical results; therefore, several attempts have already been made in this direction. Perhaps the most successful to date is by Arkilic et al. [3], who used a first-order slip model and perturbation method to solve the differential form of the Navier–Stokes and continuity equations. Their solution proceeds by first finding the lateral variation of streamwise velocity, and subsequently, the lateral velocity and streamwise variation of pressure are obtained. The obtained solution is applicable to Mach and Reynolds numbers of order epsilon (where epsilon denotes a sufficiently small number), and Knudsen number of order unity. Karniadakis and Beskok [4] used a higher order slip model but neglected the inertial terms, to derive solutions for streamwise velocity and pressure. Zohar et al. [5] also employed perturbation method on differential form of the Navier–Stokes equations. They assumed accommodation coefficient to be unity, Knudsen number of order 0.1, and neglected second order terms in the velocity slip boundary condition. Weng et al. [6] employed a high order slip model for flow in microtubes and solved the differential form of the Navier–Stokes equations along with continuity and equation of state for an ideal gas. They claimed applicability of their model for the entire range of Knudsen number, provided that the bulk velocity is negligible as compared to sonic velocity of the gas. However, there are many unknown coefficients in their slip model.

Besides the above approach of using an analytical solution starting from the Navier–Stokes equations, solution starting from Boltzmann equations has been obtained. Cercignani and Daneri [7] solved the linearized Boltzmann equation under the assumption of a small pressure gradient and isothermal condition. They used the Maxwell scattering kernel to describe the gas–wall interaction. As compared to [7], the use of variational approach by Cercignani et al. [8] leads to a slight improvement in results. Sharipov [9] also solved the linearized Boltzmann equation but used a different kernel to describe the gas–wall interaction. Comparison of the results from these analysis against experimental data showed a good agreement for $Kn < 1$, and slight deviation beyond it [7]. Xue and Fan [10] replaced Kn by a hyperbolic tangent function of Kn in the expression for slip velocity, and compared predictions from their model against computations from direct simulation Monte Carlo (DSMC). Pan et al. [11] investigated the dependence of slip coefficient on wall temperature, wall speed, and mass, diameter and number density of gas molecules for five gases, using DSMC, and found the slip coefficient to be independent of all these parameters. See Sharipov and Seleznev [12] for a recent review on internal rarefied gas flows.

The above literature survey suggests that either a first-order slip model has been employed or there is little justification for the higher-order slip model used earlier in deriving the solution of slip flow in microchannels. In this paper, analytical solution of isothermal gas flow in microchannels with slip at the walls is presented, using a second-order accurate slip model. The inertial term in the momentum equation is retained in our analysis unlike some previous studies [3,4]. The treatment is general enough to allow evaluation of the various slip models suggested in the literature [4,13], and to check the sensitivity of the results on the numerical values of the slip coefficients. Our results reduce to that of Arkilic et al. [3] upon neglecting the second-order slip term, as expected. A more general analysis such as the one employed here is expected to bring forth new insights about the flow – the new results from the analysis are highlighted at appropriate places in the paper. As mentioned above, the validity of these results extend to gaseous slip flow in both macro and micro domains provided that the underlying assumptions of flow being fully developed, steady and isothermal are satisfied.

2. Review of slip models

The no-slip boundary condition is assumed to apply at the solid-fluid interface under normal conditions. However, it is well known that at high Knudsen number this condition is violated and the gas slips at the wall. See Sandeep and Deshpande [14] for an interesting note on the no-slip boundary condition.

Maxwell proposed the following approach to calculate the slip velocity [15]. On a control surface, s, at a distance of $\lambda/2$, half of the molecules come from one mean free path away from the surface with tangential velocity u_λ, and half of the molecules are reflected from the surface. On the assumption that a fraction σ of the molecules are reflected diffusively at the walls (i.e., their average tangential velocity corresponds to that of the wall, u_w), and the remaining $(1-\sigma)$ of the molecules are reflected specularly (i.e., without a change of their impinging velocity u_λ), Maxwell obtained the following expression on expanding u_λ using Taylor series and retaining terms up to second order:

$$u_g - u_w = \frac{2-\sigma}{\sigma}\left[Kn\left(\frac{\partial u}{\partial n}\right)_s + \frac{Kn^2}{2}\left(\frac{\partial^2 u}{\partial n^2}\right)_s\right]. \quad (1)$$

In the above equation, u stands for streamwise velocity, subscripts g, w and s refer to gas, wall, and control surface respectively, σ is the tangential momentum accommodation factor ($\sigma = 1$ and 0 for fully diffused and specular surfaces, respectively), and n is the normal to the control surface.

As a somewhat arbitrary extension of the above model, Lam [16] suggested the following alternate form for ease of calculations:

$$u_g - u_w = \frac{2-\sigma}{\sigma}\left[\frac{Kn}{1-bKn}\left(\frac{\partial u}{\partial n}\right)_s\right], \quad (2)$$

where b is an empirical parameter whose value can be determined by DSMC simulations for various Knudsen number regimes. This slip model (Eq. (2)) was later exploited by Beskok and Karniadakis [17] and Karniadakis and Beskok [4], to solve for gas flow at microscales. Beskok and Karniadakis [17] determined the value b by a perturbation expansion of the velocity field in terms of Kn and have found that in the slip flow regime ($Kn \leqslant 0.1$), second order accuracy is obtained if b is chosen as:

$$b = \left[\frac{1}{2}\frac{u_o''}{u_o'}\right]_s, \quad (3)$$

where prime denotes derivative of tangential velocity in the direction normal to the surface, and the subscript "o" shows no-slip level of approximation. Using this model, Beskok and Karniadakis [17] have provided some results for transition and free-molecular regimes. As mentioned above, Xue and Fan [10] replaced Kn by $\tanh(Kn)$ and neglected the second order term in Eq. (1), to calculate their slip velocity.

Sreekanth [18] suggested the following general form of second-order slip model:

$$u_g - u_w = -C_1\lambda\left(\frac{\partial u}{\partial y}\right)_w - C_2\lambda^2\left(\frac{\partial^2 u}{\partial y^2}\right)_w,$$

which can be written as

$$u_g - u_w = -2C_1Kn\left(\frac{\partial u}{\partial n}\right)_w - 4C_2Kn^2\left(\frac{\partial^2 u}{\partial n^2}\right)_w. \quad (4)$$

This is essentially of the same form as Eq. (1) with the important difference that there are two independent coefficients unlike a single coefficient ($(2-\sigma)/\sigma$) in Eq. (1) (the factor of 2 and 4 comes into picture because of the definition of Knudsen number as $\lambda/2H$). Although there seems to be concensus on the validity of Eq. (4), there is no general agreement on the values of the slip coefficients C_1 and C_2. Table 1 summarizes the various values of the coefficients as predicted by analysis and experimental data.

The slip model (Eq. (4)) has been adopted in the present work, because it allows comparison of results from the

Table 1
Values of slip coefficients proposed in the literature

Source	C_1	C_2	Remarks
Maxwell (1879)	1	0	Theoretical (see [15])
Schamberg (1947)	1	$5\pi/12$	Theoretical (see [4])
Chapman and Cowling (1952)	≈1	≈0.5	Theoretical (see [13])
Albertoni et al. (1963)	1.1466	0	Theoretical (Pipe)
Deissler (1964)	1	1.6875	Theoretical (see [18])
Cercignani (1964)	1.1466	0.9756	Theoretical (see [18])
Sreekanth (1969)	1.1466	0.14	Experimental (Pipe)
Hsia and Domoto (1983)	1	0.5	See [4]
Mitsuya (1993)	1	2/9	See [13]
Pan et al. (1999)	1.125	0	Simulations (DSMC)

The values were obtained through theoretical considerations, DSMC simulations, or experiments. The values of Albertoni et al. [20] and Sreekanth [18] have been obtained for a circular geometry.

present theory for various values of C_1 and C_2, against available experimental data. Hence, different slip models can be compared. In this paper, we refer the slip model to be of first order if $C_2 = 0$; the slip model is of second order when both C_1 and C_2 are non-zero. Also $u_w = 0$ in our case.

According to Kennard [15], the slip length is obtained by extending the gradient at the wall to the point of zero velocity. The slip length can be determined from:

$$u_g = \zeta \frac{\partial u}{\partial y},$$

which gives

$$\zeta = C_1 Kn D_h,$$

for first order model, where ζ is the slip length, and D_h is the hydraulic diameter of the channel. Note $D_h = 2H$ in our case, where H is the distance between the two plates.

3. Solution for gas flow in microchannels

3.1. Governing equations

In this paper, we follow the approach of Sreekanth [18] to analyze gaseous slip flow in a channel under slip flow condition. The following assumptions are involved in this procedure:

- The flow is steady, two-dimensional and locally fully developed.
- The flow conditions are isothermal.
- The channel is long, and the entry and exit effects are negligible.
- The viscous compressive stresses are negligible.

Under the above assumptions, the velocity profile can be approximated by a parabola while the density (or pressure) is a function of streamwise coordinate only. The assumption of a parabolic velocity profile is shown to be true by a vast body of analysis, and experimental and numerical data available in the literature (Arkilic et al. [3], Pan et al. [11], Beskok and Karniadakis [17], Xue et al. [22], Agrawal et al. [23], Agrawal and Agrawal [24]). Similarly, the flow conditions will be close to isothermal, if the heat generated due to expansion of the gas and viscous dissipation is properly mitigated, or a good heat conductor (example silicon) is used for fabricating the microchannels [4].

The momentum balance for the case of compressible flow on a finite elemental volume between two cross sections of a channel with axial length dz is given by [18]

$$-A\mathrm{d}p - \frac{2A\tau_w}{H}\mathrm{d}z = \mathrm{d}\left[\int_A \rho u^2 \mathrm{d}A\right], \tag{5}$$

where p is pressure, and A is the cross-sectional area of the channel. It is well known (see example, Schaaf and Chambre [2], Deissler [19]) that, in the slip regime the Navier–Stokes equations are better than the Burnett equation and thirteenth-order moment equations. The caveat however is that, the equations are accurate to order Knudsen number whereas the boundary conditions have a higher order of accuracy in terms of Knudsen number (Eq. (4)); this is done with the intention of extending the applicability of the obtained solutions to larger values of Knudsen numbers. The present analysis takes into account the change in axial momentum, which is usually neglected.

Besides Navier–Stokes, the ideal gas law

$$p = \rho R T \tag{6}$$

and

$$Kn\ p = \text{constant}, \tag{7}$$

in a microchannel, will be used in the analysis. Here R is the specific gas constant and T is the absolute temperature.

3.2. Solution procedure

The essential steps for obtaining the solutions are as follows:

1. Assume a slip model (Eq. (4)) and evaluate the coefficients of the parabolic velocity profile in terms of other (known and unknown) variables. Note that the analysis can be undertaken for other slip models as well; we however choose Eq. (4) because (as mentioned above) of its general acceptability and because it allows comparison of the values of slip-coefficients from various sources in the most straightforward manner.
2. Substitute the velocity profile in the integral form of momentum equation (Eq. (5)), and solve for pressure.
3. Obtain the streamwise variation of longitudinal velocity using Eqs. (6) and (9).
4. Solve for the lateral velocity by invoking the continuity equation.
5. Calculate the mass flux, friction factor, conductance and other integral and engineering parameters of interest knowing the pressure and velocity fields.

The three coefficients of the parabola can be determined using Eq. (4), symmetry with respect to the centerline, and the local mean velocity. The velocity profile therefore becomes

$$u(y,z) = \bar{u}(z)\frac{\frac{y}{H} - \left(\frac{y}{H}\right)^2 + 2C_1 Kn + 8C_2 Kn^2}{1/6 + 2C_1 Kn + 8C_2 Kn^2}, \tag{8}$$

where y is the lateral coordinate ($=0, H$ at the lower and upper walls respectively), z is the longitudinal coordinate, and $\bar{u}$ is the cross-section averaged longitudinal velocity. Beskok and Karniadakis [17] have given the analytical velocity profile which has the same form as Eq. (8). The mean velocity is a function of the streamwise coordinate and is related to the Reynolds number through

$$Re = \frac{\rho \bar{u} D_h}{\mu}. \tag{9}$$

The numerator in Eq. (9) is equal to mass flux per unit depth and therefore the Reynolds number is invariant of streamwise location, which leads to some simplification in the analysis.

The slip velocity

$$u_g = \bar{u}\frac{2C_1Kn + 8C_2Kn^2}{1/6 + 2C_1Kn + 8C_2Kn^2},$$

indeed goes to zero as $Kn \to 0$. The contribution of second order term (i.e., $C_2 \neq 0$) to slip velocity increases at higher Kn, which suggests that they should be retained at large values of Knudsen numbers (the approximate value beyond which they should be retained will be obvious from Fig. 4 presented below). It is apparent from the above equation that the difference in velocities between the centerline and walls decreases at large Knudsen numbers, and therefore, the velocity profile appears 'flat' in such cases. Because Knudsen number is a function of streamwise location (Eq. (7)), the slip velocity is also a function of streamwise location; specifying the correct slip velocity is an important source of difficulty in numerical simulations and analytical treatment of such flows, as noted earlier. For example, Cercignani and Daneri [7] seem to have neglected the streamwise variation of slip velocity in their analysis.

The shear stress at the wall for the above velocity profile is given by

$$\tau_w = \frac{3Re\mu^2}{\rho H^2(1 + 12C_1Kn + 48C_2Kn^2)}. \tag{10}$$

We can show that the slip length for the second order system becomes [15]

$$\zeta = [C_1Kn + 4C_2Kn^2]D_h, \tag{11}$$

where, again, the second order term becomes important at high Knudsen numbers. Although Eq. (11) is a direct extension of the previous work, we believe that it has not been derived earlier for the second order system.

3.3. Solution for pressure and velocities

After substituting for u and τ_w from Eqs. (8) and (10), respectively, Eq. (5) can be integrated to obtain an expression for pressure in terms of pressure (p_0) at some reference position z_0 and the corresponding Knudsen number (Kn_0). The following expression for pressure is obtained:

$$\begin{aligned}&\left(\frac{p}{p_0}\right)^2 - 1 + 24C_1Kn_0\left(\frac{p}{p_0} - 1\right) + 96C_2Kn_0^2\log\left(\frac{p}{p_0}\right)\\ &+ 2Re^2\beta\chi\left\{12C_1Kn_0\left(\frac{p_0}{p} - 1\right) + 24C_2Kn_0^2\left[\left(\frac{p_0}{p}\right)^2 - 1\right] - \log\left(\frac{p}{p_0}\right)\right\}\\ &= -96Re\beta\frac{z - z_0}{D_h},\end{aligned} \tag{12}$$

where

$$\beta = \frac{\mu^2RT}{p_0^2D_h^2}, \tag{13}$$

$$\begin{aligned}\chi &= \frac{1}{A}\int_A\left(\frac{u}{\bar{u}}\right)^2 dA\\ &= \left[\frac{1/30 + \frac{2}{3}C_1Kn + \frac{8}{3}C_2Kn^2 + 4C_1^2Kn^2 + 32C_1C_2Kn^3 + 64C_2^2Kn^4}{(1/6 + 2C_1Kn + 8C_2Kn^2)^2}\right].\end{aligned} \tag{14}$$

Note that an assumption of constant χ was made during integration of Eq. (5) in order to simplify the algebra without compromising the accuracy of the solution [18]. It can be easily verified that χ lies between 1 and 1.17 over the range of Knudsen number from 0.001 to 10, and the maximum difference in pressure at any point with the two extreme values of χ is less than 10^{-3}%.

The variation of mean velocity can now be obtained using Eqs. (6) and (9) as:

$$\bar{u}(z) = \frac{Re\mu RT}{p(z)D_h}, \tag{15}$$

which upon using Eq. (8) gives the longitudinal velocity as

$$u(y,z) = \frac{Re\mu RT}{p(z)D_h}\left(\frac{y/H - (y/H)^2 + 2C_1Kn(z) + 8C_2Kn^2(z)}{1/6 + 2C_1Kn(z) + 8C_2Kn^2(z)}\right). \tag{16}$$

Note that $p(z)$ can be substituted from Eq. (12) in the above equations. Fig. 1a shows the longitudinal velocity for $Kn_0 = 0.0668$ and $Re = 0.0.0979$. (Unless noted otherwise, all results in this paper have been plotted for $C_1 = 1.1466$ and $C_2 = 0.9756$ and $L = 100D_h$ where L is the length of the channel). It should be noted that the variation of Knudsen number along the length of the channel has been taken into account in the above expression.

The lateral component of velocity (v) is obtained by substituting the expressions for $\rho(z)$ and $u(y,z)$ (using Eqs. (6), (12) and (16)) into the two-dimensional continuity equation:

$$\frac{\partial(\rho u)}{\partial z} + \frac{\partial(\rho v)}{\partial y} = 0. \tag{17}$$

The resulting expression for lateral velocity is

$$\begin{aligned}v(y,z) = &\frac{12C_1Kn(z) + 96C_2Kn^2(z)}{1 + 12C_1Kn(z) + 48C_2Kn^2(z)}\left(\frac{Re\mu RT}{D_h}\right)\frac{1}{p^2(z)}\\ &\times\frac{dp}{dz}\left\{y\left(1 - \frac{3\frac{y}{H} - 2\left(\frac{y}{H}\right)^2 + 12C_1Kn(z) + 48C_2(Kn(z))^2}{1 + 12C_1Kn(z) + 48C_2(Kn(z))^2}\right)\right\}.\end{aligned} \tag{18}$$

Fig. 1b shows the variation of lateral velocity for the same parameters as in Fig. 1a. It can be readily verified by comparing Fig. 1a with b that the magnitude of lateral velocity is substantially smaller (about 3 orders of magnitude for a typical microchannel) than the centerline velocity. The analysis of Arkilic et al. [3] also predicts a much smaller lateral velocity (of order epsilon) as compared to the centerline velocity.

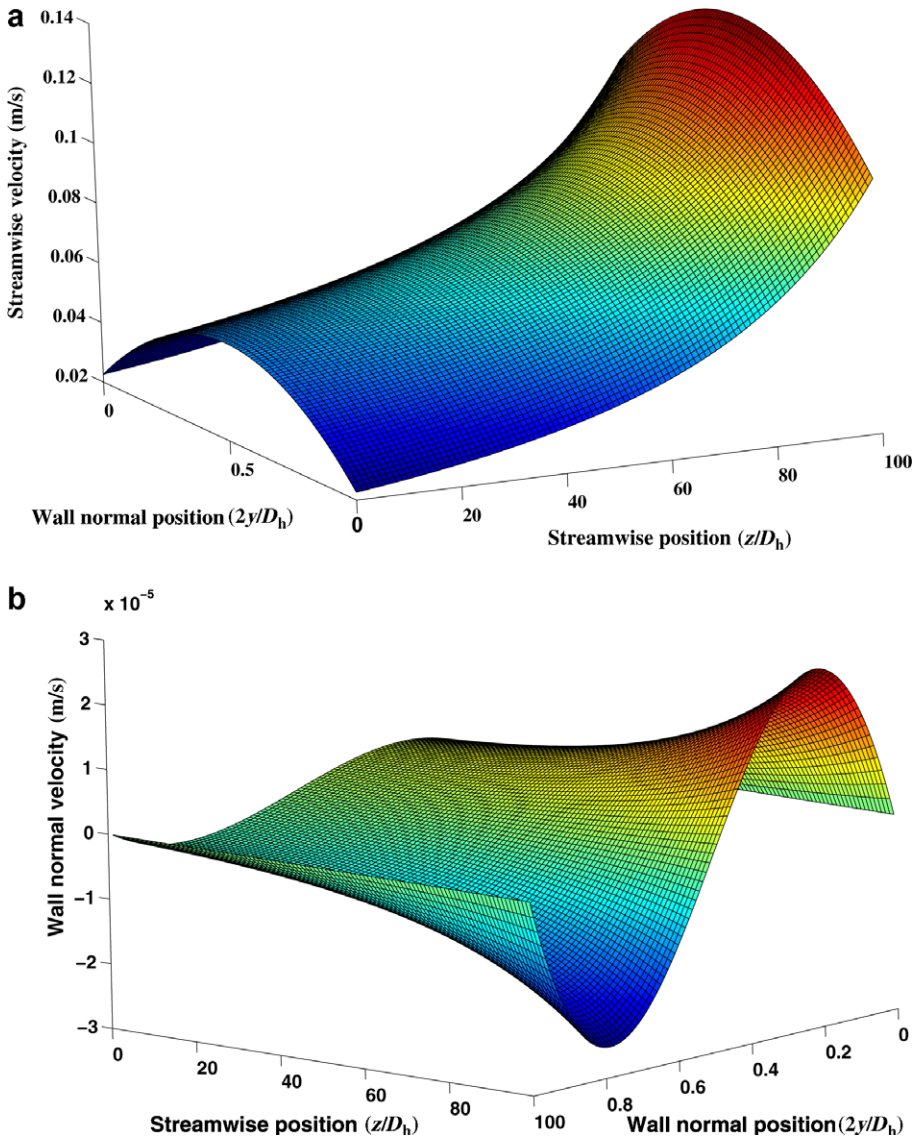

Fig. 1. Variation of (a) longitudinal and (b) lateral velocities as predicted by the theory.

3.4. Solution for integral parameters

In this section, results for some integral and engineering parameters using the results from the previous section are provided. The mass flux per unit depth through the channel is

$$\dot{m} = \int_0^H \rho u \mathrm{d}y,$$

which can be found after substituting the expressions of u and ρ. The expression for mass flux is simply,

$$\dot{m} = \frac{Re\mu}{2}. \tag{19}$$

However, in most cases, the mass flux for a prescribed pressure ratio needs to be determined. Using Eq. (12), a quadratic equation in Reynolds number is obtained; it is found that this quadratic equation has only one positive solution. The mass flow rate in terms of pressure ratio, γ, is given by

$$\dot{m} = \left[\frac{-a_2 + \sqrt{a_2^2 - 4a_1a_3}}{2a_1}\right]\frac{\mu}{2}, \tag{20}$$

where,

$$a_1 = 2\beta\chi\left[12C_1Kn_0(\gamma - 1) + 24C_2Kn_0^2(\gamma^2 - 1) + \log\gamma\right],$$
$$a_2 = 48\beta L/H, \text{ and}$$
$$a_3 = \left(\tfrac{1}{\gamma^2} - 1\right) + 24C_1Kn_0\left(\tfrac{1}{\gamma} - 1\right) - 96C_2Kn_0^2\log(\gamma).$$

For the flow of compressible gases in channels, the flow acceleration effect caused by the change of density on the total pressure drop must be considered, based on the momentum theorem, the friction factor while gas flows in a straight constant section is calculated as follows [26]:

$$\frac{\mathrm{d}p}{\mathrm{d}z} = -\frac{f}{D_h}\frac{\rho\bar{u}^2}{2} + \rho\bar{u}\frac{\mathrm{d}\bar{u}}{\mathrm{d}z}.$$

Integrating across the length of the channel and using the perfect gas equation of state, we obtain:

$$f = \left(\frac{\gamma^2 - 1}{\gamma^2}\right)\left[\frac{p_0^2 D_h^2}{4(\dot{m})^2 RT} + \log\gamma\right]\frac{2D_h}{L}. \quad (21)$$

Conductance (ϱ) of the microchannel can be defined as

$$\varrho = \frac{\dot{m}}{\Delta p},$$

(where Δp is the pressure drop across the channel) which upon using Eq. (19) and the expression for γ yields

$$\varrho = \left(\frac{\gamma}{\gamma - 1}\right)\frac{Re\mu}{2p_0}. \quad (22)$$

Conductance measurements are commonly reported in the literature; see, e.g., Tison [27].

4. Discussion

The purpose of this section is to show consistency between the obtained and previous results and to highlight new insights from the analysis.

4.1. Validation of the theory

Fig. 2 presents comparison of pressure from Eq. (12) against the experimental data of Pong et al. [25]. The measurements by [25] were made by embedding measurement ports in a microchannel through which pressure transducers were mounted. The working gas was nitrogen and the outlet Knudsen number was 0.059. The comparison between present theory and data is good.

Fig. 3 presents comparison of mass flux versus pressure ratio through the microchannel obtained from Eq. (20) against the experimental data of Arkilic et al. [3] at outlet Knudsen number of 0.155. The comparison between the theory and data is again good. Further, the second-order model is clearly an improvement over the first-order model.

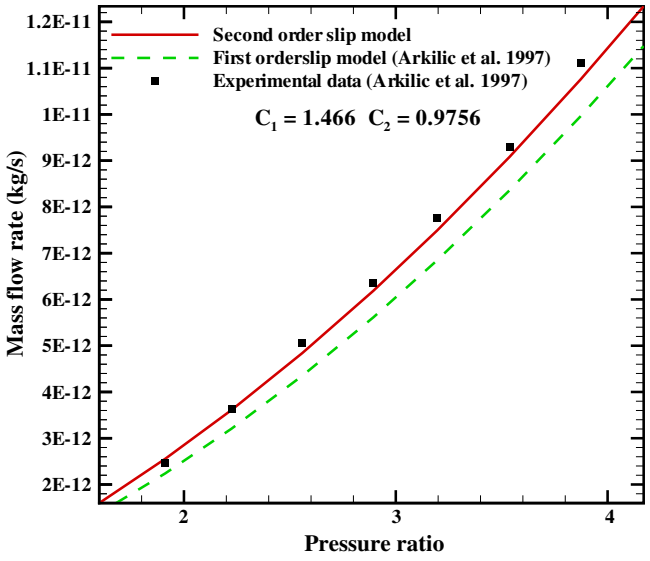

Fig. 3. Comparison of mass flux against experimental data of Arkilic et al. [3], for outlet Knudsen number of 0.155.

Fig. 4 presents comparison of normalized volume flux versus Knudsen number through the microchannel obtained from the present theory against the analysis of Cercignani and Daneri [7] and Cercignani et al. [8]. Also shown is the experimental data of Dong for five different gases, obtained from Ref. [7]. The normalized volume flux is obtained as

$$Q = \frac{-\rho c_s \int_0^H U\,dy}{H^2(dp/dz)}, \quad (23)$$

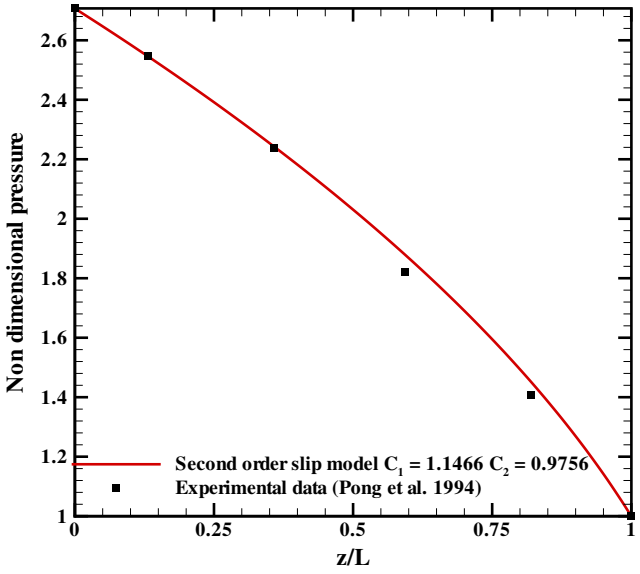

Fig. 2. Comparison of pressure against experimental data of Pong et al. [25], for outlet Knudsen number of 0.059.

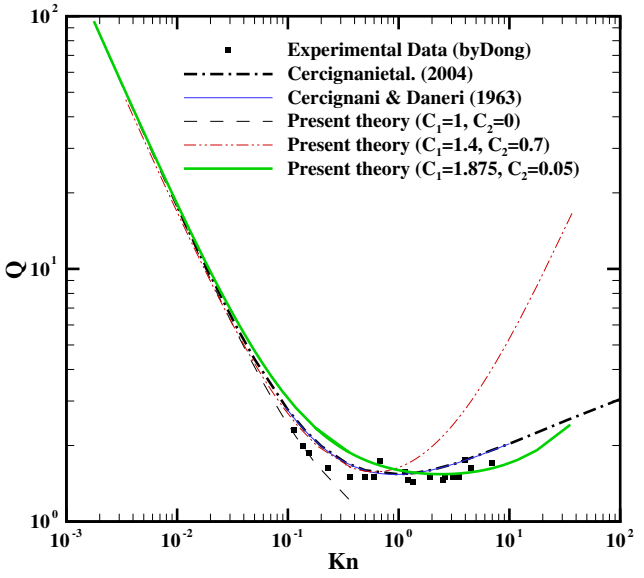

Fig. 4. Comparison of normalized volume flux versus Knudsen number, against the theoretical results obtained by Cercignani et al. [7,8].

where c_s is the speed of sound. Our expression with $C_1 = 1$ and $C_2 = 0$ agrees well with Cercignani et al. [7,8] for Kn less than about 0.1, which corresponds roughly to the end of the slip flow regime. The comparison can however be improved by choosing $C_2 > 0$, and changing the value of C_1 slightly, i.e., by using any of the values of C_2 given in Table 1 (not shown; to avoid overcrowding the figure). In particular, the comparison between the two theories is excellent till $Kn \approx 1$ with $C_1 = 1.4$ and $C_2 = 0.7$. Similarly, reasonable comparison up to $Kn = 5$ is obtained by choosing $C_1 = 1.875$ and $C_2 = 0.05$. Sreekanth [18] had noted that comparison between his experimental data and the theory derived by him improves by changing the values of C_1 and C_2, from 1 and 0 for $Kn \leqslant 0.03$, to 1.1466 and 0 for $0.03 < Kn < 0.13$, and to 1.1466 and 0.14 for $Kn \geqslant 0.13$. This observation justifies to some extend, using different values of C_1 and C_2 in different Knudsen number regimes.

The values of C_1 and C_2 employed above are artificial, in the sense that these values have not been reported earlier. However, on using these values, Fig. 4 reveals that results from theory based on continuum assumptions can be matched with that from the Boltzmann equation for a sufficiently large range of Knudsen number; this result is important from the point-of-view of numerical simulation of rarefied gases. In other words, Fig. 4 suggests that theory based on continuum assumptions in conjunction with a higher order boundary condition and an appropriate choice of the slip coefficients can be employed even at high Knudsen numbers, when the use of continuum assumptions are themselves questionable. Further evidence and similar results in other geometries, will open the exciting possibility of studying a large part of rarefied gases with the Navier–Stokes equations itself, for which simulation and analysis tools are perhaps better developed than with the Boltzmann equation.

The results in this section show that the present theory is consistent with previous experimental data and theoretical analysis. Further, they underscore the utility of employing a higher order slip model for the analysis of rarefied gases. In the following section, we show that our expression for pressure and velocity will reduce to Arkilic et al. [3] upon neglecting the second order term. This further establishes that our results are consistent, rather more general, than the existing models.

4.2. Reduction to first order slip expression

On differentiating Eq. (12) twice, with respect to z and substituting $C_2 = 0$, we obtain:

$$\frac{\partial^2}{\partial z^2}\left(\frac{p}{p_0}\right)^2 + \frac{24C_1Kn_0}{p_0}\frac{\partial^2 p}{\partial z^2} + 2Re^2\beta\chi\left(\frac{24C_1Kn+1}{p^2}\left[\frac{\partial p}{\partial z}\right]^2 - \frac{12C_1Kn+1}{p}\frac{\partial^2 p}{\partial z^2}\right) = 0, \tag{24}$$

which can be compared to the corresponding expression by Arkilic et al. [3]

$$\frac{\partial^2}{\partial z^2}\left(\frac{p}{p_0}\right)^2 + \frac{24C_1Kn_0}{p_0}\frac{\partial^2 p}{\partial z^2} = 0. \tag{25}$$

(Note that the coefficient of $\partial^2 p/\partial z^2$ in Eq. (25) has changed from that in Ref. [3] because of our definition of Kn as $\lambda/2H$ instead of λ/H used therein.) The extra term in Eq. (24) – $2Re^2\beta\chi\{(\frac{24C_1Kn+1}{p^2})(\frac{\partial p}{\partial z})^2 - (\frac{12C_1Kn+1}{p})\frac{\partial^2 p}{\partial z^2}\}$, appears because the entire analysis is second order accurate; the magnitude of this term is dependent on the square of Reynolds number. However, if Reynolds and Knudsen numbers are of order epsilon and unity, respectively, the coefficient of the extra term (i.e., $2Re^2\beta\chi$) is epsilon square (this can be easily verified – β lies between 0.1 and 10 while χ is of order unity as noted earlier), and therefore it is substantially smaller than the other terms. That is, under the assumptions made by Arkilic et al. [3], the magnitude of the extra term is negligible, and Eq. (24) indeed reduces to Eq. (25). (The negligible difference between the two equations under the above assumption is illustrated through a specific example in Fig. 5a.) However, in general, pressure in microchannel is dependent on both Reynolds and Knudsen numbers, with a more dominant effect of the latter non-dimensional number. The dependence on Reynolds number was not reported earlier because the inertial terms were neglected in the previous analysis [3,4]. It is however expected that this term will become important in rarefied gas flow in macrochannels [18].

An analysis similar to pressure can be performed for velocity, and a reduction to first order expression can be demonstrated upon neglecting the extra term given above. The good agreement with Ref. [3] is demonstrated for a particular case in Fig. 5b. This shows that, because our expression can be reduced to Arkilic et al. [3], which employs only a first-order slip boundary condition and is accurate only to order epsilon (first term in the perturbation analysis), our results can be considered to be more general.

4.3. Comparison of first-order and second-order slip models

The effect of rarefaction on pressure distribution was assessed by varying the Knudsen number [4]. Fig. 6a shows a decrease in non-linearity with an increase in Knudsen number up to $Kn \approx 0.16$. At $Kn = 0.16$, the pressure distribution becomes linear, and beyond it, the curvature changes from convex with respect to the origin, to concave. The curvature increases between $Kn = 0.16$ and $Kn = 3.34$ before decreasing. Eq. (12) further suggests that at very large Knudsen numbers, pressure again becomes almost linear, in agreement with the limiting case of free-molecular flows; however, the validity of the analysis is questionable beyond Kn of order unity, because the continuum assumption used in derivation of Navier–Stokes equations is perhaps not valid.

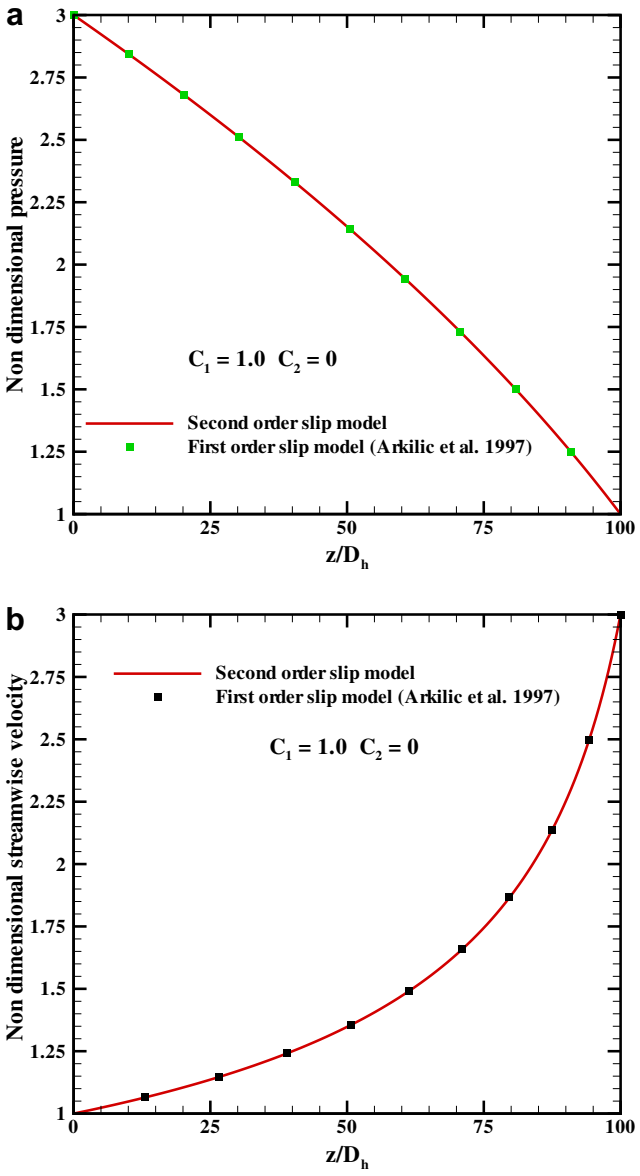

Fig. 5. Reduction of the present theory to first-order and comparison against the predictions of Arkilic et al. [3] for (a) pressure, and (b) velocity ($Kn_0 = 0.068$, $Re = 0.0745$).

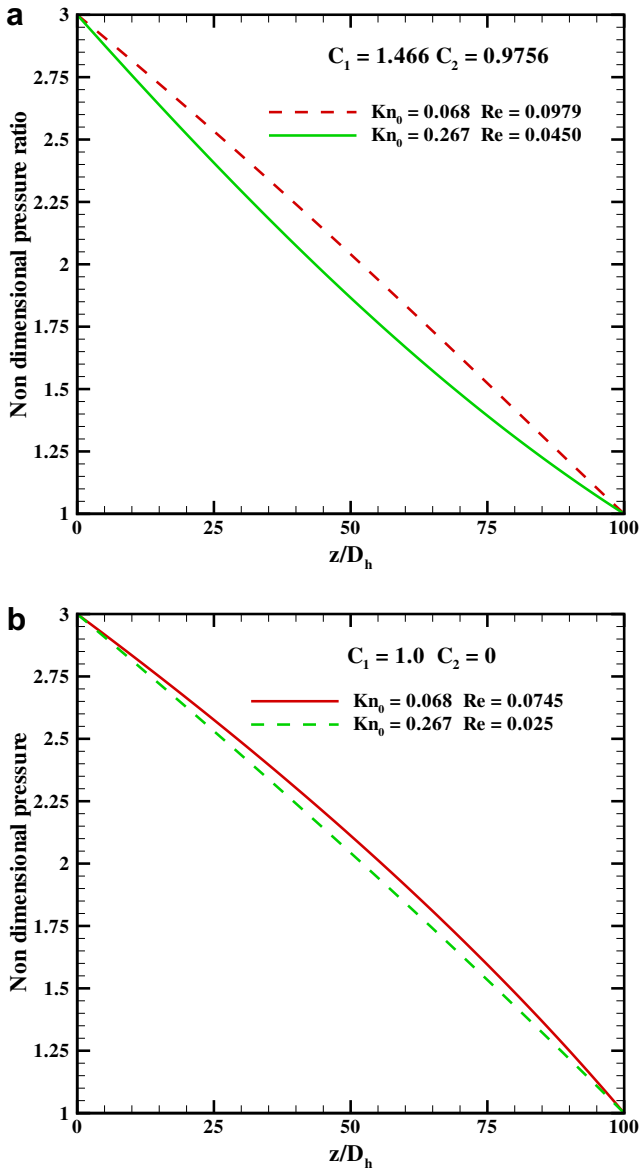

Fig. 6. Effect of Knudsen number on pressure distribution obtained from (a) second-order, and (b) first-order models. Note the change in curvature in the top figure.

An interesting comparison for pressure can be made against result from first order theory which fails to show a change in curvature with Knudsen number (Fig. 6b). This motivated us to derive the condition at which the curvature will go to zero as

$$\frac{1}{p_0^2} - \frac{48C_2Kn_0^2}{p^2} + Re^2\beta\chi\left(\frac{24C_1Kn_0p_0}{p^3} + 1\right) = 0. \tag{26}$$

The above equation was obtained by differentiating Eq. (12) twice with respect to z and substituting $\partial^2 p/\partial z^2 = 0$. The only way to satisfy Eq. (26) is to have $C_2 > 0$ (the positive sign before the first and third terms makes these terms positive, and the equation can not go to zero without an equal and opposite contribution from the second term). It is noted that all the values of C_2 suggested in Table 1 are positive. In other words, a first order analysis (with $C_2 = 0$) will not show a change in curvature for pressure. A change in curvature has been seen in the numerical simulations of Nie et al. [28] at a comparable Knudsen number (=0.194).

On plotting the volume flux through a capillary against the mean pressure driving the flow, Knudsen found a peculiar behaviour. The volume flux first decreases with an increase in mean pressure, before increasing. In other words, there is a minima in volume flux, which is rather paradoxical, and is referred to as the "Knudsen's paradox". Subsequent experiments have confirmed this observation and several theoretical attempts have been made to explain the phenomena. Note however that the mass flux versus Knudsen number will not show any such minima.

The interest here is in comparing the first and second order theories in predicting this paradoxical behaviour.

Fig. 4 shows a minima in volume flux with the second order analysis, but not with the first order analysis. In order words, the volume flux increases monotonically with mean pressure when $C_2 = 0$, irrespective of the value of C_1. The result is significant in that it shows that a slip model has to be at least second order accurate before the Knudsen's minima will be observed; conversely, a model which captures the above minima would be at least second order accurate.

5. Conclusions

An analytical study of gas flow through microchannels has been presented in this paper. The analysis employs integral form of the Navier–Stokes equations which are assumed to be valid in the slip-flow regime, and a second-order slip model was used to compute the slip velocity. The exact expressions for pressure and velocities are derived for this important class of flows. The derived expressions are in terms of the slip coefficients; comparison of results for predicted slip coefficients against experimental data, allows evaluation of different slip models proposed in the literature. These results are also applicable to rarefied gas in a macrochannel.

The theory is validated against experimental data available in the literature. We also show that the prediction from the theory using standard values of the slip coefficients compares well against Cercignani's linearized Boltzmann equation based calculations till Knudsen number of 0.1, which corresponds to the limit of the slip flow regime. However, the comparison between the two theories can be improved by tuning the values of the slip coefficients. We have been able to demonstrate agreement between results from Navier–Stokes and Boltzmann equations up to Knudsen number of around five for flow in a channel; at such high Knudsen numbers the former equation is normally considered not applicable.

The study documents the variation of pressure and velocity in the channel for different values of Knudsen number. A peculiar behaviour – change in curvature of pressure versus the streamwise coordinate at high Knudsen numbers is observed and explained for the first time. On plotting the normalized volume flux versus Knudsen number, the presence of Knudsen's minima is correctly predicted by the results, which is another important validation test for a new theory. Finally, some important differences in the prediction from first-order and second-order analysis are pointed out – change in curvature of pressure and Knudsen's minima can only be predicted with the higher order model.

Because of the difficulty in making precise measurements, simulation should be the more commonly used approach to study gas flows through microchannels. Importance of our results lies in the fact that they suggest: first, Navier–Stokes equations along with second order slip model and appropriate coefficients can be used for simulating a sufficiently large range of Knudsen number, and second, any simulation which wants to capture behaviour of pressure and volume flux correctly, should employ at least second order accurate boundary condition.

Acknowledgements

We are grateful to Mr. G. Sultania for independently verifying some of the results presented in this paper. Also thanks to Dr. S.V. Prabhu for discussion and other help. A part of this work was presented at the 33rd National and 3rd International Conference on Fluid Mechanics and Fluid Power held at IIT Bombay between 7–9 December 2006 as paper no. NCFMFP2006-1505.

References

[1] M. Gad-el-Hak, The fluid mechanics of microdevices – The Freeman scholar lecture, J. Fluids Eng. 121 (1999) 5–33.
[2] S.A. Schaaf, P.L. Chambre, Flow of rarefied gases, Princeton University Press, NJ, 1961.
[3] E.B. Arkilic, M.A. Schimidt, K.S. Breuer, Gaseous slip flow in long micro-channels, J. Microelectromech. Syst. 6 (1997) 167–178.
[4] G.E. Karniadakis, A. Beskok, Microflows – Fundamentals and simulations, Springer-Verlag, New York, 2002.
[5] Y. Zohar, S.Y.K. Lee, W.Y. Lee, L. Jiang, P. Tong, Subsonic gas flow in a straight and uniform microchannel, J. Fluid Mech. 472 (2002) 125–151.
[6] C.I. Weng, W.L. Li, C.C. Hwang, Gaseous flow in microtubes at arbitrary Knudsen numbers, Nanotechnology 10 (1999) 373–379.
[7] C. Cercignani, A. Daneri, Flow of a rarefied gas between two parallel plates, J. Appl. Phys. 34 (1963) 3509–3513.
[8] C. Cercignani, M. Lampis, S. Lorenzani, Variational approach to gas flows in microchannels, Phys. Fluids 16 (2004) 3426–3437.
[9] F. Sharipov, Application of the Cercignani–Lampis scattering kernel to calculations of rarefied gas flows. I. Plane flow between two parallel plates, Eur. J. Mech. B 21 (2002) 113–123.
[10] H. Xue, Q. Fan, A high order modification on the analytic solution of 2-D microchannel gaseous flow, in: Proc. of ASME 2000 Fluids Eng. Division Summer Meeting, Boston, June.
[11] L.S. Pan, G.R. Liu, K.Y. Lam, Determination of slip coefficient for rarefied gas flows using direct simulation Monte Carlo, J. Micromech. Microeng. 9 (1999) 89–96.
[12] F. Sharipov, V. Seleznev, Data on internal rarefied gas flows, J. Phys. Chem. Ref. Data 27 (1998) 657–706.
[13] S. Colin, Rarefaction and compressibility effects on steady and transient gas flows in microchannels, Microfluid. Nanofluid. 1 (2005) 268–279.
[14] P. Sandeep, M.D. Deshpande, A note on the no-slip boundary condition, Report no. PD-CF-0304, National Aerospace Laboratories, Bangalore, India (2003).
[15] E.H. Kennard, Kinetic theory of gases with an introduction to statistical mechanics, Allied Pacific, Bombay (1962).
[16] See Professor A. Beskok's website: http://www.cfm.brown.edu/people/beskok/lam.slip.html.
[17] A. Beskok, G.E. Karniadakis, A model for flows in channels, pipes, and ducts at micro and nano scales, Microscale Thermophys. Eng. 3 (1999) 43–77.
[18] A.K. Sreekanth, Slip flow through long circular tubes, in: L. Trilling, H.Y. Wachman (Eds.), Proceedings of the sixth international symposium on Rarefied Gas Dynamics, Academic Press, 1969, pp. 667–680.
[19] R.G. Deissler, An analysis of second-order slip flow and temperature-jump boundary conditions for rarefied gases, Int. J. Heat Mass Transfer 7 (1964) 681–694.

[20] S. Albertoni, C. Cercignani, L. Gotusso, Numerical Evaluation of the slip coefficient, Phys. Fluids 6 (1963) 993–996.
[21] Y. Mitsuya, Modified Reynolds equation for ultra-thin film gas lubrication using 1.5-order slip-flow model and considering surface accommodation coefficient, J. Tribol. 115 (1993) 289–294.
[22] H. Xue, Q. Fan, C. Shu, Prediction of micro-channel flows using direct simulation Monte Carlo, Probab. Eng. Mech. 15 (2000) 213–219.
[23] A. Agrawal, L. Djenidi, R.A. Antonia, Simulation of gas flow in microchannels with a sudden expansion or contraction, J. Fluid Mech. 530 (2005) 135–144.
[24] A. Agrawal, A. Agrawal, Three-dimensional simulation of gas flow in different aspect ratio microducts, Phys. Fluids 18 (2006) 103604.
[25] K. Pong, C.M. Ho, J. Liu, Y.C. Tai, Non-linear pressure distribution in uniform microchannels, in: Proc. of Appl. Microfabrication to Fluid Mech., ASME Winter Annual Meeting, Chicago, (1994). pp. 51–56.
[26] P. Wu, W.A. Little, Measurement of friction factors for the flow of gases in very fine channels used for microminiature Joule–Thompson refrigerators, Cryogenics 23 (1983) 273–277.
[27] S.A. Tison, Experimental data and theoretical modeling of gas flows through metal capillary leaks, Vacuum 44 (1993) 1171–1175.
[28] X. Nie, G.D. Doolen, S. Chen, Lattice-Boltzmann simulations of fluid flows in MEMS, J. Statist. Phys. 107 (2002) 279–289.